CrystEngComm

PAPER

View Article Online
View Journal | View Issue

Open Access Article. Published on 11 September 2017. Downloaded on 12/4/2025 7:41:17 PM.
This article is licensed under a Creative Commons Attribution-NonCommercial 3.0 Unported Licence.

Check for updates

Cite this: *CrystEngComm*, 2017, **19**, 5797

A series of Cd(II) coordination polymers based on flexible bis(triazole) and multicarboxylate ligands: topological diversity, entanglement and properties†

Ke Li,[a] Vladislav A. Blatov,[bc] Tao Fan,[c] Tian-Rui Zheng,[a] Ya-Qian Zhang,[a] Bao-Long Li *[a] and Bing Wu[a]

Eight Cd(II) coordination polymers, $\{[Cd(btrb)(H_2O)_4][Cd_2(btrb)(btec)(H_2O)_2]_2(OH)_2\cdot 5H_2O\}_n$ (**1**·$(OH)_2\cdot 5H_2O$), $\{[Cd(btrb)_{0.5}(bptc)_{0.5}]\cdot H_2O\}_n$ (**2**·H_2O), $\{[Cd_3(btrb)(btc)_2]\cdot 3H_2O\}_n$ (**3**·$3H_2O$), $\{[Cd(btrb)(ip)(H_2O)]\cdot H_2O\}_n$ (**4**), $\{[Cd(btrb)(MeOip)]\cdot H_2O\}_n$ (**5**), $\{[Cd_2(btrb)_2(1,2\text{-}bdc)_2]\cdot 3H_2O\}_n$ (**6**), $\{[Cd_2(btrb)(bpdc)_2]_2\cdot 11H_2O\}_n$ (**7**) and $\{[Cd(btrb)(bpdc)]\cdot H_2O\}_n$ (**8**), were synthesized under hydrothermal conditions. **1** shows an unprecedented (4,4,4,4)-connected 3D (electroneutral motif) + 1D (cationic motif) → 3D polythreaded structure. The point symbol of the new 3D motif is $(4^6)_2(8^6)(4^2\cdot 8^2\cdot 10^2)(4^3\cdot 8^3)_4$, or the second **mot** topology based on the $[Cd_2(COO)]$ dimer. **2** shows an unprecedented (4,5,6)-connected 3D network with a point symbol of $(4^2\cdot 8^4)(4^7\cdot 6^3)_2(4^6\cdot 6^6\cdot 8^3)$. **3** shows an unprecedented (3,8)-connected self-catenated 3D network based on the Cd(II) trimer cluster $[Cd_3(COO)_2]$ with a point symbol of $(4^2\cdot 6)_2(4^4\cdot 6^{11}\cdot 7^6\cdot 8^6\cdot 9)$. **4** exhibits a 2D + 2D → 2D interpenetration network based on the 2D **sql** network. **5** exhibits a 4-connected network with a **cds** topology. **6** presents the first example of a 2-fold interpenetrating 6-connected **cco-6-*Pbcm*** 3D network with a point symbol of $(4^7\cdot 6^8)$. **7** shows a (3,3,4,4)-connected 2D 3,3,4,4L72 network with a point symbol of $(3\cdot 4\cdot 5)(4\cdot 8^2)(3\cdot 4\cdot 5\cdot 8^3)(3\cdot 4\cdot 8^2\cdot 9^2)$. **8** presents a (3,5)-connected self-catenated 2D 3,5L2 network with a point symbol of $(4^2\cdot 6)(4^2\cdot 6^7\cdot 8)$. The luminescence and thermal stability of **1**–**8** were investigated.

Received 25th June 2017,
Accepted 10th September 2017

DOI: 10.1039/c7ce01176h

rsc.li/crystengcomm

Introduction

The synthesis of coordination polymers (CPs) with specific structures is still a great challenge, and has been a hot topic in chemistry for decades due to not only the interesting topologies, but also the multitudinous properties for functional materials in various fields, such as gas adsorption and storage, catalysis, sensors, luminescent materials and so on.[1–6] The well-known TOPOS topological databases contain more than 180 000 types of topology and more than 1 700 000 examples of their occurrences in crystal structures.[7,8] Topological analysis of crystal structures can help us better understand the structural features of coordination polymers and allow us to compare them with other coordination polymers. In order to pre-design the synthesis of coordination polymers with specific structures, a good understanding of the structural features of the coordination polymers is necessary.

The entanglements of coordination polymers are particularly intriguing because of the presence of periodic entanglements, in which independent motifs are entangled together in different modes. Entangled networks can be classified as interpenetrated, polycatenated, polythreaded or polyknotted.[9–12] Interpenetrated and polycatenated networks are the two most common entangled systems, but self-catenated coordination networks are uncommon and less exploited.[9,10] Polythreaded structures are characterized by the presence of closed loops, as well as elements that can thread through the loops, and can be considered as extended periodic analogues of molecular rotaxanes and pseudo-rotaxanes.[11,12] The few polythreaded species include 0D → 1D or 2D, 1D → 2D or 1D → 3D, 1D + 2D → 2D, 1D + 2D → 3D, 2D → 3D, and 1D + 3D → 3D.[11,12] Polythreaded structures with 3D components are really rare.[12]

The assembly of CPs is controlled by numerous factors under hydrothermal conditions, such as temperature, the ratio of materials, ligands, pH, solvent and other factors.[13] The

[a] *State and Local Joint Engineering Laboratory for Functional Polymeric Materials, College of Chemistry, Chemical Engineering and Materials Science, Soochow University, Suzhou 215123, PR China. E-mail: libaolong@suda.edu.cn*
[b] *Samara Center for Theoretical Materials Science (SCTMS), Samara University, Ac. Pavlov St. 1, Samara 443011, Russia*
[c] *School of Materials Science and Engineering, Northwestern Polytechnical University, Xi'an, Shaanxi 710072, PR China*

† Electronic supplementary information (ESI) available: PXRD patterns, TGA curve and additional figures. CCDC 1554826–1554833. For ESI and crystallographic data in CIF or other electronic format see DOI: 10.1039/c7ce01176h

Open Access Article. Published on 11 September 2017. Downloaded on 12/4/2025 7:41:17 PM.
This article is licensed under a Creative Commons Attribution-NonCommercial 3.0 Unported Licence.

carboxyl group has flexible coordination modes with metal ions. The various coordination modes of the carboxyl group can be divided into three modes: monodentate, bridging and chelating. 1-Substituted 1,2,4-triazole ligands are widely used in the construction of CPs or MOFs, while 4-substituted 1,2,4-triazole ligands are still less used. The 1,2-nitrogen atoms of 4-substituted 1,2,4-triazole ligands make them strong σ-donors when coordinating with one or two metal ions. The co-ligand (N-donor and carboxylate ligands) system is the most popular way to design, synthesize and regulate CPs and MOFs.[14] The combination of multicarboxylate and 1,2,4-triazole co-ligands is a very effective method in the construction and regulation of CPs. Our group focuses on the design and synthesis of novel CPs and MOFs with intriguing topologies and interesting properties, using multicarboxylate ligands and imidazole or triazole co-ligands.[15] For example, three MOFs based on a $[Co_4(\mu_3\text{-}OH)_2]$ cluster were synthesized and connected numbers of $[Co_4(\mu_3\text{-}OH)_2]$ clusters from 4 to 6 and then 8 were successfully regulated.[15d] In this work, we focus on the construction and regulation of Cd(II) CPs with intriguing topologies and interesting properties using the 4-substituted bis(1,2,4-triazole) ligand 1,4-bis(1,2,4-triazol-4-ylmethyl)benzene (btrb) and multicarboxylate co-ligands. Eight Cd(II) CPs, $\{[Cd(btrb)(H_2O)_4][Cd_2(btrb)(btec)(H_2O)_2]_2(OH)_2\cdot 5H_2O\}_n$ (**1**·$(OH)_2$·$5H_2O$), $\{[Cd(btrb)_{0.5}(bptc)_{0.5}]\cdot H_2O\}_n$ (**2**·H_2O), $\{[Cd_3(btrb)(btc)_2]\cdot 3H_2O\}_n$ (**3**·$3H_2O$), $\{[Cd(btrb)(ip)(H_2O)]\cdot H_2O\}_n$ (**4**), $\{[Cd(btrb)(MeOip)]\cdot H_2O\}_n$ (**5**), $\{[Cd_2(btrb)_2(1,2\text{-}bdc)_2]\cdot 3H_2O\}_n$ (**6**), $\{[Cd_2(btrb)(bpdc)_2]_2\cdot 11H_2O\}_n$ (**7**) and $\{[Cd(btrb)(bpdc)]\cdot H_2O\}_n$ (**8**), were synthesized under hydrothermal conditions (btrb = 1,4-bis(1,2,4-triazol-4-ylmethyl)-benzene, H_4btec = 1,2,4,5-benzene tetracarboxylic acid, H_4bptc = (1,1′-biphenyl)tetracarboxylic acid, H_3btc = 1,3,5-benzenetricarboxylic acid, H_2ip = isophthalic acid, H_2MeOip = 4-methoxyl-isophthalic acid, 1,2-H_2bdc = phthalic acid, H_2-bpdc = (1,1′-biphenyl)-2,2′-dicarboxylic acid). **1** presents an unprecedented (4,4,4,4)-connected 3D (electroneutral motif) + 1D (cationic motif) → 3D polythreaded network with a *bli1* topology, where the point symbol of the 3D motif is $(4^6)_2(8^6)(4^2\cdot 8^2\cdot 10^2)(4^3\cdot 8^3)_4$, or a second **mot** topology based on the $[Cd_2(COO)]$ dimer. **2** shows an unprecedented 3D (4,5,6)-connected *bli2* topology with a point symbol of $(4^2\cdot 8^4)(4^7\cdot 6^3)_2(4^6\cdot 6^6\cdot 8^3)$. **3** shows an unprecedented 3D (3,8)-connected *bli3* topology based on the Cd(II) trimer cluster $[Cd_3(COO)_2]$ with a point symbol of $(4^2\cdot 6)_2(4^4\cdot 6^{11}\cdot 7^6\cdot 8^6\cdot 9)$. **4–8** show topologies devisable by the regulation of the multicarboxylate ligands. The luminescence and thermal stability were investigated.

Experimental

Materials and methods

1,4-Bis(1,2,4-triazol-4-ylmethyl)benzene (btrb) was synthesized according to the reported method.[16] All reagents were purchased and used without further purification. Elemental analyses for C, H and N were performed on a Perkin-Elmer 240C analyzer. FT-IR spectra were obtained on a Bruker VERTEX 70 FT-IR spectrophotometer in the 4000–600 cm^{-1} region. Powder X-ray diffraction (PXRD) was performed on a D/MAX-3C diffractometer with Cu-Kα radiation (λ = 1.5406 Å) at room temperature. Thermogravimetric analysis (TGA) was carried out using a Thermal Analyst 2100 TA Instrument and SDT 2960 Simultaneous TGA-DTA Instrument with nitrogen flow at a heating rate of 10 °C min^{-1}. The luminescence measurements were carried out in the solid state at room temperature and the spectra were collected on a PerkinElmer LS50B spectrofluorimeter.

Synthesis of $\{[Cd(btrb)(H_2O)_4][Cd_2(btrb)(btec)(H_2O)_2]_2(OH)_2\cdot 5H_2O\}_n$ (**1**·$(OH)_2$·$5H_2O$)

A mixture of H_4btec (0.04 mmol, 0.010 g), $CdSO_4$·8/3H_2O (0.06 mmol, 0.015 g) in 7.5 mL H_2O and btrb (0.4 mmol, 0.096 g) in 0.4 mL DMF was adjusted to pH = 8 with dilute NaOH solution. The mixture was added to a 25 mL Teflon-lined stainless autoclave, sealed and then heated at 110 °C for 3 days, then left for one month at room temperature to give colourless block crystals of **1**·$(OH)_2$·$5H_2O$ (yield: 0.014 g, 34% based on H_4btec). Anal. calc. for $C_{56}H_{68}Cd_5N_{18}O_{31}$ (**1**·$(OH)_2$·$5H_2O$): C, 32.79; H, 3.34; N, 12.29%; found: C, 32.70; H, 3.41; N, 12.19%. IR (cm^{-1}): 3370 (m), 1580 (s), 1538 (vs), 1489 (m), 1423 (m), 1371 (vs), 1207 (w), 1079 (w), 995 (w), 873 (w), 815 (w), 743 (w), 625 (m).

Synthesis of $\{[Cd(btrb)_{0.5}(bptc)_{0.5}]\cdot H_2O\}_n$ (**2**·H_2O)

A mixture of H_4bptc (0.025 mmol, 0.008 g), $CdSO_4$·8/3H_2O (0.05 mmol, 0.013 g) in 7.5 mL H_2O and btrb (0.05 mmol, 0.012 g) in 0.5 mL DMF was adjusted to pH = 7 with dilute NaOH solution. The mixture was added to a 25 mL Teflon-lined stainless autoclave, sealed and then heated at 90 °C for 3 days, then cooled to room temperature. Colourless stick crystals of **2**·H_2O were obtained (yield: 0.017 g, 42% based on btrb). Anal. calc. for $C_{14}H_{11}CdN_3O_5$(**2**·H_2O): C, 40.65; H, 2.68; N, 10.16%; found: C, 41.39; H, 2.57; N, 10.32%. IR (cm^{-1}): 3389 (w), 1585 (vs), 1539 (s), 1361 (vs), 1159 (s), 1067 (m), 1022 (m), 864 (vs), 831 (s), 791 (s), 727 (s), 667 (s), 627 (vs).

Synthesis of $\{[Cd_3(btrb)(btc)_2]\cdot 3H_2O\}_n$ (**3**·$3H_2O$)

The synthesis procedure for **3** is similar to that for **2**, except that H_3btc (0.04 mmol, 0.008 g) was used instead of H_4bptc. Colourless block crystals of **3**·$3H_2O$ were obtained (yield: 0.014 g, 27% based on btrb). Anal. calc. for $C_{30}H_{24}Cd_3N_6O_{15}$ (**3**·$3H_2O$): C, 34.45; H, 2.31; N, 8.03%; found: C, 34.61; H, 2.31; N, 7.96%. IR (cm^{-1}): 3369 (m), 3102 (w), 1612 (s), 1526 (s), 1434 (s), 1369 (vs), 1213 (w), 1108 (w), 1071 (w), 1028 (w), 765 (s), 720 (vs), 633 (s).

Synthesis of $\{[Cd(btrb)(ip)(H_2O)]\cdot H_2O\}_n$ (**4**)

The synthesis procedure for **4** is similar to that for **2**, except that H_2ip (0.05 mmol, 0.008 g) was used instead of H_4bptc. Colourless block crystals of **4** were obtained (yield: 0.022 g, 80% based on btrb). Anal. calc. for $C_{20}H_{20}CdN_6O_6$ (**4**): C,

 This journal is © The Royal Society of Chemistry 2017

Open Access Article. Published on 11 September 2017. Downloaded on 12/4/2025 7:41:17 PM.
This article is licensed under a Creative Commons Attribution-NonCommercial 3.0 Unported Licence.

43.41; H, 3.62; N, 15.20%; found: C, 43.24; H, 3.73; N, 15.11%. IR (cm^{-1}): 3324 (m), 3122 (w), 1655 (w), 1609 (m), 1542 (s), 1371 (s), 1181 (m), 1075 (m), 1010 (m), 764 (m), 723 (s), 628 (s).

Synthesis of $\{[Cd(btrb)(MeOip)]\cdot H_2O\}_n$ (5)

The synthesis procedure for **5** is similar to that for **2**, except that H_2MeOip (0.05 mmol, 0.010 g) was used instead of H_4-bptc. Colourless block crystals of **5** were obtained (yield: 0.018 g, 64% based on btrb). Anal. calc. for $C_{21}H_{20}CdN_6O_6$ (**5**): C, 44.62; H, 3.54; N, 14.87%; found: C, 44.41; H, 3.67; N, 14.69%. IR (cm^{-1}): 3421 (m), 3116 (w), 1611 (m), 1562 (s), 1449 (w), 1420 (m), 1377 (s), 1258 (s), 1188 (w), 1136 (w), 1076 (m), 1019 (m), 897 (w), 864 (w), 835 (w), 782 (m), 716 (s), 684 (m), 638 (vs).

Synthesis of $\{[Cd_2(btrb)_2(1,2\text{-bdc})_2]\cdot 3H_2O\}_n$ (6)

The synthesis procedure for **6** is similar to that for **2**, except that 1,2-H_2bdc (0.05 mmol, 0.008 g) was used instead of H_4-bptc. Colourless block crystals of **6** were obtained (yield: 0.024 g, 88% based on btrb). Anal. calc. for $C_{40}H_{38}Cd_2N_{12}O_{11}$ (**6**): C, 44.13; H, 3.49; N, 15.45%; found: C, 43.95; H, 3.62; N, 15.33%. IR (cm^{-1}): 3320 (m), 3110 (w), 1690 (w), 1538 (vs), 1442 (w), 1363 (vs), 1212 (vs), 1161 (m), 1076 (m), 1016 (m), 887 (m), 859 (m), 830 (m), 754 (s), 710 (s), 633 (s).

Synthesis of $\{[Cd_2(btrb)(bpdc)_2]_2\cdot 11H_2O\}_n$ (7)

The synthesis procedure for **7** is similar to that for **2**, except that H_2bpdc (0.05 mmol, 0.012 g) was used instead of H_4-bptc. Colourless block crystals of **7** were obtained (yield: 0.024 g, 46% based on btrb). Anal. calc. for $C_{80}H_{78}Cd_4N_{12}O_{27}$ (**7**): C, 45.99; H, 3.76; N, 8.05%; found: C, 45.87; H, 3.83; N, 7.93%. IR (cm^{-1}): 3387 (m), 1603 (w), 1533 (vs), 1439 (m), 1396 (vs), 1192 (w), 1080 (w), 860 (m), 752 (s), 719 (s), 706(s), 685 (s), 669 (s), 631 (s).

Synthesis of $\{[Cd(btrb)(bpdc)]\cdot H_2O\}_n$ (8)

The synthesis procedure for **8** is similar to that for **2**, except that H_2bpdc (0.03 mmol, 0.007 g) was used instead of H_4-bptc. Colourless plate crystals of **8** were obtained (yield: 0.012 g, 39% based on btrb). Anal. calc. for $C_{26}H_{22}CdN_6O_5$ (**8**): C, 51.12; H, 3.63; N, 13.76%; found: C, 51.01; H, 3.85; N, 13.61%. IR (cm^{-1}): 3466 (m), 3094 (w), 1690 (w), 1612 (m), 1549 (vs), 1466 (w), 1394 (vs), 1190 (m), 1067 (m), 1013 (m), 962 (w), 905 (w), 837 (m), 814 (m), 768 (s), 741 (m), 723 (m), 677 (m), 636 (s).

X-ray crystallography

X-ray diffraction data were collected on a Rigaku Saturn 724 CCD, Agilent Gemini Atlas or Bruker D8 Quest diffractometer with graphite monochromated Mo-Kα radiation (λ = 0.71073 Å). The intensities were collected by ω-scan and reduced on the *CrystalClear* (Rigaku Inc., 2007), *CrysAlisPro* (Agilent Technologies, 2013) or *APEX III* (Bruker Corp., 2016) program. A multi-scan absorption correction was applied.[17] The positions of the hydrogen atoms were determined by theoretical calculations. The structures were solved and refined by the *SHELXTL* package.[18] The solvent molecules in **1**, **2** and **3** were removed with the *SQUEEZE* procedure in *PLATON*.[19] The *ISOR* and *EADP* commands were used and the occupancies of the disordered atoms were determined to make sure that the U_{eq} values were reasonable. The number of lattice water molecules for **1**, **2** and **3** was deduced from the TGA and elemental analysis. The parameters of the crystal data collection and refinement are given in Table S1.† Selected bond lengths, bond angles and hydrogen bonds are given in Tables S2 and S3 in the ESI.†

Results and discussion

Synthesis of 1–8

The balanced chemical reaction equations of **1**–**8** are shown in Fig. S43 in the ESI.† **2**–**8** were all prepared under common hydrothermal conditions, while **1** could not be obtained in the same way. During the preparation of **1**, we found that the btec ligand has a very strong bonding ability with Cd(II) atoms, even stronger than the btrb ligand under hydrothermal conditions. We could only obtain $[Cd(btec)_{0.5}(H_2O)]_n$ (CCDC: 214511)[20] at certain ratios and temperatures (from 70 °C to 140 °C). $[Cd(btec)_{0.5}(H_2O)]_n$ is still the only product except the unknown precipitate, even when the ratio of btrb : btec = 10 : 1. In order to get a CP in which btrb and btec ligands both coordinate with Cd(II) atoms, we tried to use $[Cd(btec)_{0.5}(H_2O)]_n$ as the starting material. Crystals of $[Cd(btec)_{0.5}(H_2O)]_n$ were put into a solution of btrb. After leaving the solution to stand for a long time, the shape of the $[Cd(btec)_{0.5}(H_2O)]_n$ crystals changed from diamond-like to big blocks, suggesting the formation of **1**. Then we improved the steps in the preparation as shown in the synthesis section by a combination of the hydrothermal method and solvent method. This case shows a step-synthesis strategy in a mixed ligand system, especially for those ligands which have big differences in coordination ability. The crystals can be constructed by the metal and strong ligands first and then these crystals can be used as a material to react with a solution of the weak ligand under suitable conditions. There is a good chance of obtaining unexpected products after the reaction. The combination of the hydrothermal/solvothermal method and solvent method is a new thinking in the preparation of unusual CPs.

Crystal structure of $\{[Cd(btrb)(H_2O)_4][Cd_2(btrb)(btec)(H_2O)_2]_2(OH)_2\cdot 5H_2O\}_n$ (1 $\cdot(OH)_2\cdot 5H_2O$)

1 is composed of a 3D electroneutral motif and a 1D cationic motif polythreaded together and forms a 1D + 3D → 3D polythreaded network. The 3D motif shows an unprecedented (4,4,4,4)-connected *bli1* topology or a second **mot** topology based on the $[Cd_2(COO)]$ dimer. The asymmetric unit of the 3D motif consists of two Cd(II) atoms (Cd1/Cd2), two halves

Open Access Article. Published on 11 September 2017. Downloaded on 12/4/2025 7:41:17 PM.
This article is licensed under a Creative Commons Attribution-NonCommercial 3.0 Unported Licence.

of btec ligands, one btrb ligand and two coordinated water molecules. Cd1 is in a distorted octahedral geometry, coordinated by three carboxylate oxygen atoms (O1/O2/O8A) from two btec ligands, two nitrogen atoms (N1/N5B) from two btrb ligands and one water oxygen atom (O9). Cd2 is in a 7-coordinated pentagonal bipyramidal geometry, coordinated by four carboxylate oxygen atoms (O1/O3/O5/O6) from two btec ligands, two nitrogen atoms (N2/N4B) from two btrb ligands and one water oxygen atom (O10) (Fig. S1 in the ESI†). Two kinds of btec ligand are both coordinated with four Cd(II) atoms in three kinds of coordination mode: chelating bridging (O1O2), monodentate (O3O4/O8O7) and chelating (O5O6) modes (Fig. S2 and S3 in the ESI†). The btrb ligands are all coordinated with four Cd(II) atoms in a *cis*-configuration. Two btrb ligands (N1–N6/N1B–N6B) connected with the same four Cd(II) atoms form a $[Cd_4(btrb)_2]$ ring (Fig. S4 in the ESI†). The planes of the benzene rings in the coordination ring are parallel, with a distance of 3.2 Å. The $[Cd_4(btrb)_2]$ rings are linked by btec ligands and extended to form a nano-tunnel (Fig. 1a, Fig. S5 in the ESI†). The distance between the adjacent parallel nano-tunnels is 13.2 Å. The adjacent nano-tunnels are connected by btec ligands to form a unique 3D network (Fig. 1b). The planes formed by the adjacent parallel nano-tunnels are also parallel, with a distance of 9.8 Å, and the space angle of the nano-tunnels in adjacent planes is 70.5° along the *c*-axis.

Topologically, the Cd1 and Cd2 atoms are both coordinated by two btrb and two btec ligands. Two kinds of btec ligand and the btrb ligands in the 3D motif are all coordinated by four Cd(II) atoms. Thus, the Cd(II) atoms and the btec and btrb ligands can all be described as 4-connected nodes. The structure of the 3D motif is analysed with Toptware.[7] The 3D network in **1** can be simplified as a (4,4,4,4)-connected network (Fig. 1c) with a point symbol of $(4^6)_2(8^6)(4^2{\cdot}8^2{\cdot}10^2)(4^3{\cdot}8^3)_4$.[21]

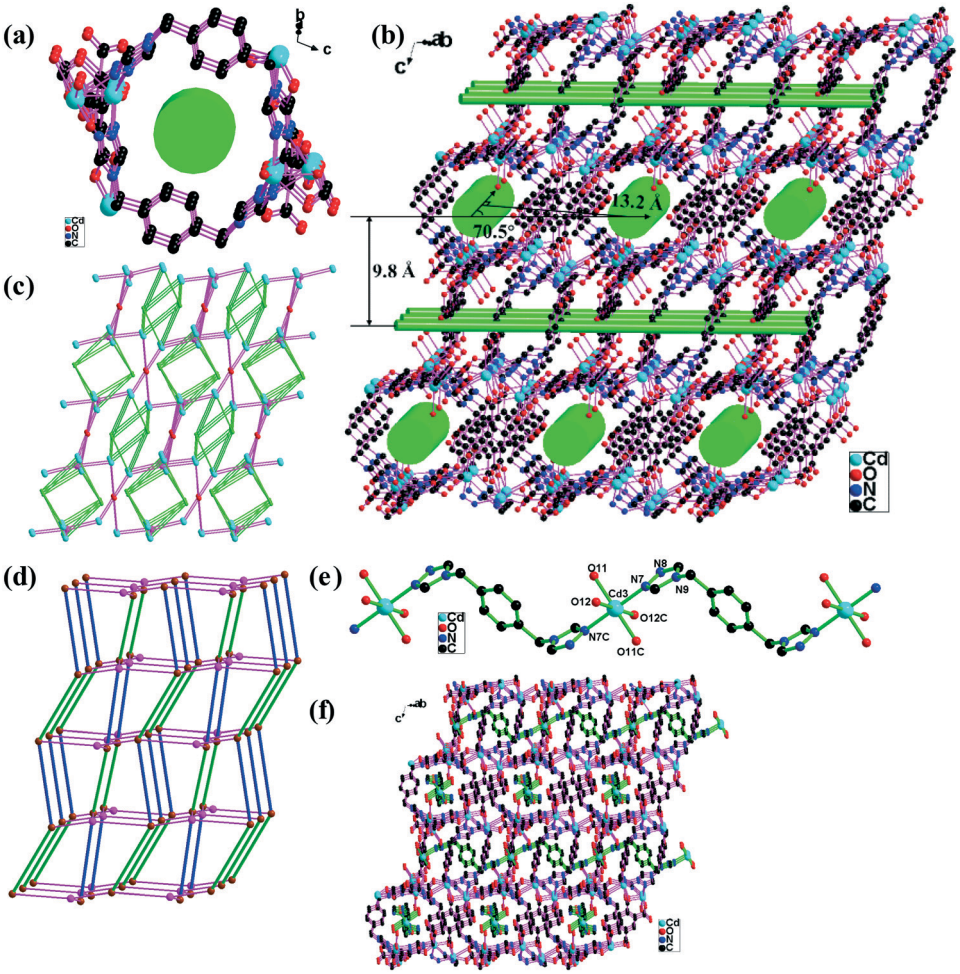

Fig. 1 (a) The nano-tunnel in **1**; (b) the 3D motif in **1**. The bright green cylinders represent the 1D nano-tunnels; (c) schematic depiction of the (4,4,4,4)-connected 3D network in **1**. The bright green, red, pink and turquoise balls represent the 4-connected btrb, btec (O1–O4) and btec (O5–O8) ligands and 4-connected Cd(II) atoms; (d) schematic depiction of the (4,4)-connected **mot** network based on the $[Cd_2(COO)]$ dimer in **1**. The pink and brown balls represent the 4-connected btec (O5–O8) ligands and 4-connected $[Cd_2(COO)]$ dimers, respectively. The bright green and blue sticks represent 2-connected double btrb and btec (O1–O4) ligands, respectively; (e) the 1D cationic motif in **1**; (f) the 1D + 3D → 3D polythreaded network of **1**.

Open Access Article. Published on 11 September 2017. Downloaded on 12/4/2025 7:41:17 PM.
This article is licensed under a Creative Commons Attribution-NonCommercial 3.0 Unported Licence.

This topology is unprecedented, and was deposited in the TTD (Topos Topological Database) collection and named *bli1*.[7]

To simplify the topologies, if the $[Cd_2(COO)]$ dimer is simplified as a 4-connected node, the double btrb ligands in the $[Cd_4(btrb)_2]$ ring and the btec (O1–O4) ligand are all 2-connected. The btec (O5–O8) ligand can also be considered as a 4-connected node. The 3D structure can be simplified as a (4,4)-connected **mot** topology with a point symbol of $(6^4 \cdot 8^2)_2(6^6)$ (Fig. 1d). According to the TTO (Topological Types Observed) collection, only one example of the **mot** topology has been reported before.[22]

The asymmetric unit of the 1D cationic motif consists of half of a Cd(II) atom (Cd3), half of a btrb ligand and two water molecules (Fig. 1e). The btrb ligands connect the adjacent Cd(II) atoms to form a 1D cationic chain $\{[Cd(btrb)(H_2O)_4]^{2+}\}_n$ with a Cd···Cd distance of 14.5113(31) Å. The disordered hydroxyl ions balance the charge. The 1D cationic chains pass through the nano-tunnels in the 3D motif to form a 1D + 3D → 3D polythreaded network (Fig. 1e). Hydrogen bonding interactions stabilize the polythreading array (Table S3 in the ESI†). The solvent accessible volume calculated by *PLATON* is 1391.8 Å^3, which is 18.6% of the cell volume. The disordered hydroxyl ions and lattice water molecules are located in the void.

Polythreaded structures with finite components are unusual. Polythreaded networks containing 3D components are really rare.[9–12] To the best of our knowledge, examples involving 3D component polythreaded frameworks have only rarely been reported. The Wang group reported five polyoxometalate-based polythreaded structures involving 3D components.[12a–c] $[Cu(bbi)_2V_{10}O_{26}][Cu(bbi)]_2 \cdot H_2O$,[12a] $[Cu^{II}(bbi)_2(\alpha\text{-}Mo_8O_{26})][Cu^{I}(bbi)]_2$, $[Cu^{II}Cu^{I}(bbi)_3(\alpha\text{-}Mo_8O_{26})][Cu^{I}(bbi)]$,[12b] $[Cu^{I}(bix)][(Cu^{I}bix)(\delta\text{-}Mo_8O_{26})_{0.5}]$ and $H(Cu^{I}bix)[(CuIbix)_2(\beta\text{-}Mo_8O_{26})] \cdot 2H_2O$ (bbi = 1,1′-(1,4-butanediyl)bis(imidazol), bix = 1,4-bis(imidazol-1-ylmethyl)benzene)[12c] exhibit similar 1D + 3D → 3D polythreaded networks based on a 3D polyoxometalate anionic network and 1D cationic chains. Our group synthesized three 1D + 3D → 3D polythreaded networks, which were all constructed by a 3D anionic network and 1D cationic chains.[12d–f]

In short, the interesting structural features of **1** can be summarized as three aspects: (a) **1** shows a rare 1D + 3D → 3D polythreaded structure; (b) **1** is the first 1D + 3D → 3D polythreaded structure which is constructed by a 3D electroneutral network (not a 3D anionic network) and 1D cationic chains; (c) the 3D electroneutral network exhibits an unprecedented (4,4,4,4)-connected network.

Crystal structure of $\{[Cd(btrb)_{0.5}(bptc)_{0.5}] \cdot H_2O\}_n$ (2·H_2O)

2 shows an unprecedented (4,5,6)-connected network. The asymmetric unit of **2** consists of one Cd(II) atom, half of a btrb ligand and half of a bptc ligand. Cd1 is in a distorted pentagonal bipyramidal geometry and coordinates five carboxylate oxygen atoms (O1/O1A/O2A/O3/O3B) from three bptc ligands and two nitrogen atoms (N1/N2A) from two btrb ligands (Fig. S6 in the ESI†). The bptc ligands in **2** show chelating bridging and bridging coordination modes with six Cd(II) atoms (Fig. S7 in the ESI†). The Cd(II) atoms are connected by the bptc ligands and extend to form a $[Cd(bptc)_{0.5}]_n$ 2D network (Fig. 2a). Each btrb ligand shows an *anti*-conformation and coordinates four Cd(II) atoms with its 1,2-position triazole nitrogen atoms (Fig. S8 in the ESI†). The $[Cd(bptc)_{0.5}]_n$ 2D networks are linked by btrb ligands and construct a 3D network (Fig. 2b).

Topologically, each Cd(II) atom is coordinated by three bptc ligands and two btrb ligands and can be described as a 5-connected node (Fig. S9 in the ESI†), while the bptc ligands and btrb ligands are 6-connected and 4-connected nodes, respectively (Fig. S7 and S8 in the ESI†). The 3D structure of **2** can be simplified as a (4,5,6)-connected network (Fig. 2c) with a point symbol of $(4^2 \cdot 8^4)(4^7 \cdot 6^3)_2(4^6 \cdot 6^6 \cdot 8^3)$.[21] This topology is unprecedented, and was deposited in the TTD (Topos Topological Database) collection and named *bli2*.[7]

Crystal structure of $\{[Cd_3(btrb)(btc)_2] \cdot 3H_2O\}_n$ (3·3H_2O)

3 presents an unprecedented (3,8)-connected 3D network based on the Cd(II) trimer cluster $[Cd_3(COO)_2]$. The asymmetric unit consists of one (Cd2) and half (Cd1) Cd(II) atoms, half

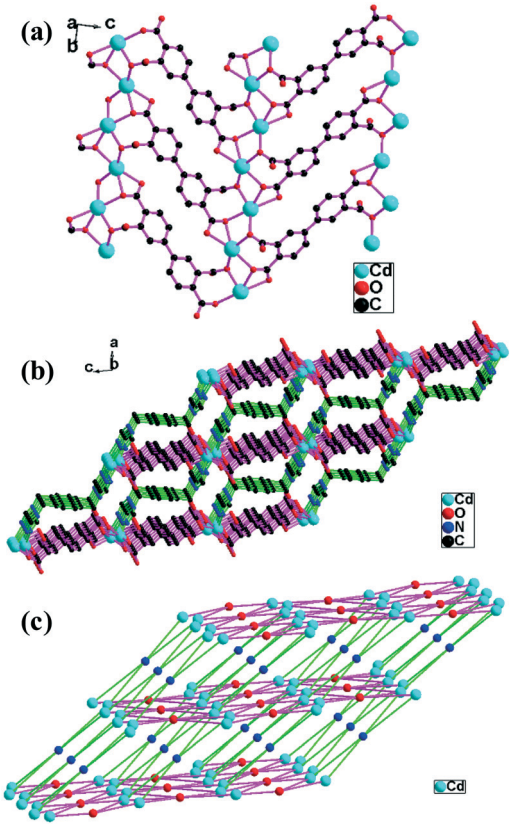

Fig. 2 (a) The $[Cd(bptc)_{0.5}]_n$ 2D network in **2**; (b) the 3D network in **2**; (c) schematic depiction of the (4,5,6)-connected 3D network of **2**. The blue and red balls represent the 4-connected btrb ligands and 6-connected bptc ligands. The turquoise balls represent 5-connected Cd(II) atoms.

Open Access Article. Published on 11 September 2017. Downloaded on 12/4/2025 7:41:17 PM.
This article is licensed under a Creative Commons Attribution-NonCommercial 3.0 Unported Licence.

of a btrb ligand (N1–N3) and one btc ligand (O1–O6). Cd1 coordinates with four carboxylate oxygen atoms (O1/O1C/O6A/O6B) from four btc ligands and two nitrogen atoms (N1/N1C) from two btrb ligands in a distorted octahedral geometry. The Cd2 atom is in a distorted octahedral geometry coordinating with five carboxylate oxygen atoms (O1/O2/O3D/O4D/O5B) from three btc ligands and one nitrogen atom (N2) from one btrb ligand (Fig. S10 in the ESI†). One btc ligand is coordinated with five Cd(II) atoms. The three carboxylate groups show three kinds of coordination mode: bidentate bridging for O1O2, bidentate chelating for O3O4 and a bidentate coordination mode for O5O6 (Fig. S11 in the ESI†). The O1 carboxylate oxygen atoms and the O1C atoms from the two btc ligands show a bridging mode and connect two Cd(II) atoms. The Cd(II) trimer cluster $[Cd_3(COO)_2]$ is formed. The Cd(II) trimer clusters $[Cd_3(COO)_2]$ are joined by btc ligands and the $[Cd_3(btc)_2]_n$ 3D network is formed (Fig. 3a). Each btrb ligand shows an *anti*-conformation and connects four Cd(II) atoms. The Cd(II) atoms of the $[Cd_3(btc)_2]_n$ 3D network are linked by btrb ligands and the $[Cd_3(btrb)(btc)_2]_n$ 3D network is constructed (Fig. 3b).

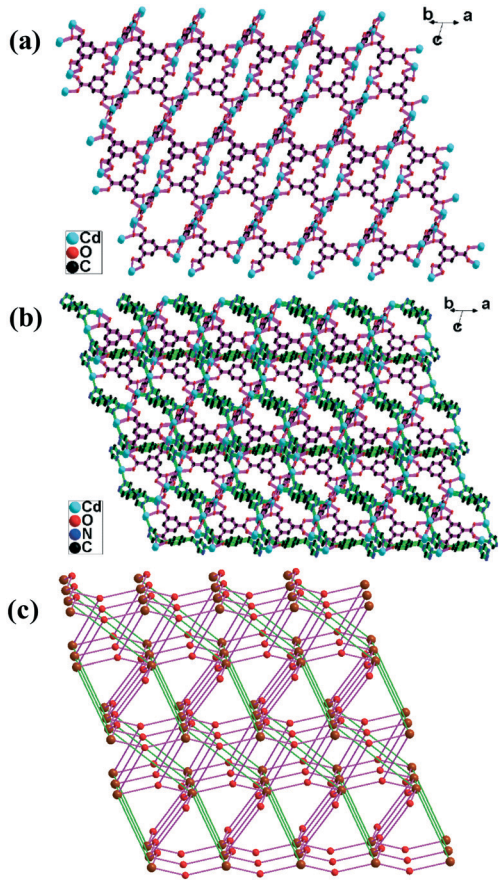

Fig. 3 (a) The $[Cd_3(btc)_2]_n$ 3D network in **3**; (b) the $[Cd_3(btrb)(btc)_2]_n$ 3D network in **3**; (c) schematic depiction of (3,8)-connected network of **3**. The red and brown balls represent the 3-connected btc ligands and 8-connected $[Cd_3(COO)_2]$ clusters. The bright green sticks represent 2-connected btrb ligands.

Topologically, if the Cd(II) trimer cluster $[Cd_3(COO)_2]$ is simplified as one node, it connects six btc ligands and two btrb ligands and is 8-connected (Fig. S12 in the ESI†). Each btc ligand coordinates three $[Cd_3(COO)_2]$ and is 3-connected. Each btrb ligand links two $[Cd_3(COO)_2]$ and is 2-connected. The 3D network of **3** can be simplified as a (3,8)-connected network (Fig. 3c) with a point symbol of $(4^2{\cdot}6)_2(4^4{\cdot}6^{11}{\cdot}7^6{\cdot}8^6{\cdot}9)$.[21] This topology is unprecedented, and was deposited in the TTD (Topos Topological Database) collection and named *bli3*.[7] The network is a self-catenated 3D network. Self-catenated 3D networks are unusual and few have been reported in the literature.[21] The solvent accessible volume calculated by *PLATON* excluding water molecules is 927.9 Å^3, which is 24.6% of the cell volume.

Crystal structure of $\{[Cd(btrb)(ip)(H_2O)]{\cdot}H_2O\}_n$ (4)

4 exhibits a 2D + 2D → 2D interpenetration network based on an undulated 2D **sql** network. The asymmetric unit consists of one Cd(II) atom, two halves of btrb ligands, one ip ligand, one coordinated water molecule and one lattice water molecule. Cd1 is 6-coordinated with three carboxylate oxygen atoms (O1/O2/O4A) from two ip ligands, two nitrogen atoms (N1/N4) from two btrb ligands and one water molecule in a distorted octahedral geometry (CdO_4N_2) (Fig. S13 in the ESI†).

The btrb ligands exhibit an *anti*-configuration and are 2-connected. Two carboxylate groups of one ip ligand act as monodentate and chelating modes (Fig. S14 in the ESI†). The 2-connected btrb and ip ligands connect the 4-connected Cd(II) nodes to form an undulated 2D **sql** network (Fig. 4a) with a point symbol of $(4^4{\cdot}6^2)$. Two adjacent undulated 2D networks interpenetrate each other and a 2D + 2D → 2D interpenetration network is formed (Fig. 4b).

Crystal structure of $\{[Cd(btrb)(MeOip)]{\cdot}H_2O\}_n$ (5)

5 exhibits a 4-connected 3D network. **5** crystallizes in the monoclinic system with a $P2_1/n$ space group. The asymmetric unit consists of one Cd(II) atom, two halves of btrb ligands, one MeOip ligand and one lattice water molecule. Cd1 is 5-coordinated with three carboxylate oxygen atoms (O1/O2/

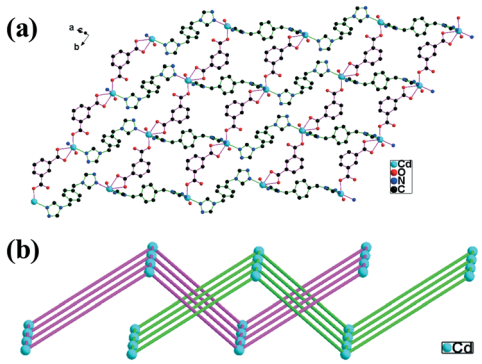

Fig. 4 (a) The 2D network of **4**; (b) the 2D + 2D → 2D interpenetration network in **4**.

Open Access Article. Published on 11 September 2017. Downloaded on 12/4/2025 7:41:17 PM.
This article is licensed under a Creative Commons Attribution-NonCommercial 3.0 Unported Licence.

O3A) from two MeOip ligands and two nitrogen atoms from two btrb ligands (N2/N4) in a distorted square pyramidal geometry (CdO_3N_2) (Fig. S15 in the ESI†). The structural distortion index τ for the Cd1 atom is 0.288, indicating that the coordination environment of the metal atom is closer to a square pyramidal geometry than a trigonal bipyramidal configuration.

Two carboxylate groups of one MeOip ligand act as chelating (O1O2) and monodentate (O3O4) modes. The MeOip ligands are 2-connected. The Cd···Cd distance separated by the MeOip bridge is 8.9586(26) Å. The btrb ligands exhibit an *anti*-configuration and are 2-connected. Each Cd(II) atom connects four other Cd(II) atoms through two MeOip and two btrb bridges. The Cd···Cd distances separated by the btrb bridges are 14.5312(40) and 13.9854(33) Å. The Cd(II) atoms are connected by MeOip and btrb ligands and extend to construct a self-catenated 3D network (Fig. 5a).

Topologically, each Cd(II) is 4-connected. The MeOip and btrb ligands are 2-connected. The 3D network of **5** can be simplified as a 4-connected 3D network of a **cds** topology (Fig. 5b) with a point symbol of ($6^5 \cdot 8$).

Crystal structure of $\{[Cd_2(btrb)_2(1,2\text{-bdc})_2]\cdot 3H_2O\}_n$ (6)

6 presents a 6-connected 3D **cco-6-*Pbcm*** network. The asymmetric unit of **6** consists of two Cd(II) atoms, one btrb ligand and two halves of btrb ligands, two 1,2-bdc ligands and three lattice water molecules. Cd1 is in a distorted octahedral geometry coordinated with three carboxylate oxygen atoms (O1/O3/O5C) from two 1,2-bdc ligands and three nitrogen atoms (N1/N8/N11B) from three btrb ligands. Cd2 is in a distorted pentagonal bipyramidal geometry coordinated with four carboxylate oxygen atoms (O1/O2/O7/O8) from two 1,2-bdc ligands and three nitrogen atoms (N4/N7/N12B) from three btrb ligands (Fig. S16 in the ESI†). Two kinds of btrb ligand (N1–N3/N4–N6) act as 2-connected bridges and coordinate two Cd(II) atoms (Fig. S17 in the ESI†). The third kind of btrb ligand (N7–N12) coordinates four Cd(II) atoms with its 1,2-position triazole nitrogen atoms (Fig. S18 in the ESI†). There are two kinds of 1,2-bdc ligand. One kind of 1,2-bdc ligand (O1–O4) shows a chelating bridging (O1O2) and monodentate (O3O4) mode (Fig. S19 in the ESI†). The other kind of 1,2-bdc ligand (O5–O8) shows a monodentate (O5O6) and chelating (O7O8) coordination mode (Fig. S20 in the ESI†).

A 1,2-bdc ligand (O1–O4) bridges the Cd1 and Cd2 atoms and forms the $[Cd_2(1,2\text{-bdc})]$ dimer. The $[Cd_2(1,2\text{-bdc})]$ dimer is linked by a 1,2-bdc ligand (O5–O8) and constructs the $[Cd_2(1,2\text{-bdc})_2]_n$ 1D chain (Fig. S21 in the ESI†). The $[Cd_2(1,2\text{-bdc})_2]_n$ 1D chains are connected by btrb ligands and form the 3D network (Fig. 6a).

Topologically, if the $[Cd_2(1,2\text{-bdc})]$ dimer is simplified as one node, it connects two 1,2-bdc ligands and four btrb ligands and is a 6-connected node (Fig. S22 in the ESI†). The

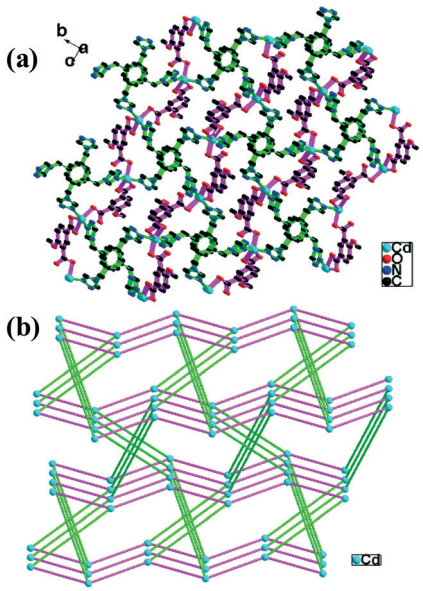

Fig. 5 (a) The 3D network of **5**; (b) schematic depiction of the 4-connected 3D network in **5**. The pink and bright green sticks represent MeOip and btrb ligands, respectively.

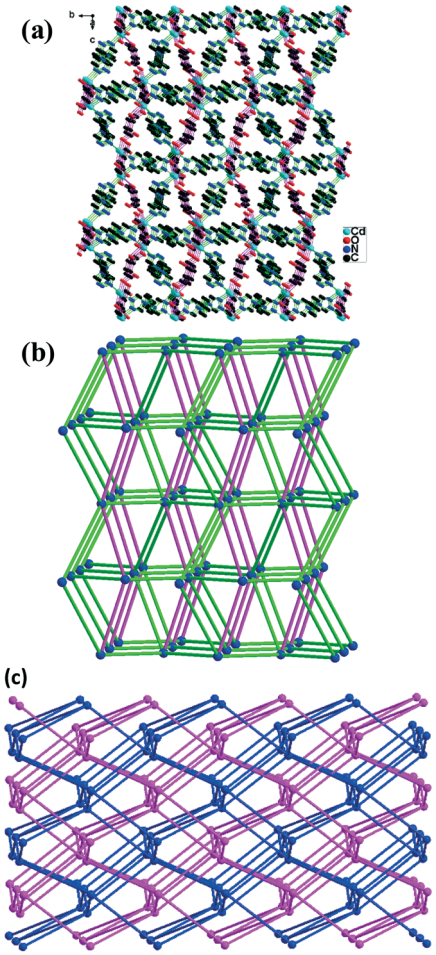

Fig. 6 (a) The 3D network of **6**; (b) schematic depiction of the 6-connected 3D network in **6**. The blue balls represent the 6-connected $[Cd_2(1,2\text{-bdc})]$ dimers. The bright green and pink sticks show the 2-connected btrb and 2-connected 1,2-bdc (O5–O8) ligands. (c) The 2-fold interpenetrating **cco-6-*Pbcm*** motifs in **6**.

Open Access Article. Published on 11 September 2017. Downloaded on 12/4/2025 7:41:17 PM.
This article is licensed under a Creative Commons Attribution-NonCommercial 3.0 Unported Licence.

1,2-bdc ligands (O5–O8) and btrb ligands are 2-connected. The 3D structure of **6** can be simplified as a 6-connected 3D **cco-6-*Pbcm*** network with a point symbol of $(4^7{\cdot}6^8)$ (Fig. 6b).[21] According to the TTO Collection, there are just two examples of this topology among CPs formed by dimeric structural groups,[23] but **6** contains two interpenetrating **cco-6-*Pbcm*** motifs (Fig. 6c) and is the first such example for this topology.

Crystal structure of $\{[Cd_2(btrb)(bpdc)_2]_2{\cdot}11H_2O\}_n$ (7)

7 shows a (3,3,4,4)-connected 2D network. The asymmetric unit of **7** consists of two Cd(II) atoms, one btrb ligand, two bpdc ligands, three ordered lattice water molecules and two and a half disordered lattice water molecules. Cd1 is in a distorted octahedral geometry coordinated with four carboxylate oxygen atoms (O1/O3/O5A/O6A) from two bpdc ligands and two nitrogen atoms (N1/N4B) from two btrb ligands. Cd2 is seven coordinated with six carboxylate oxygen atoms (O1C/O2C/O3/O4/O7/O8) from three bpdc ligands and one nitrogen atom (N2) from one btrb ligand (Fig. S23 in the ESI†).

There are two kinds of bpdc ligand, one of which shows a dual bidentate bridging mode (O1O2/O3O4) and coordinates with three Cd(II) atoms (Fig. S24 in the ESI†). The other shows a dual chelating (O5O6/O7O8) coordination mode and coordinates with two Cd(II) atoms (Fig. S25 in the ESI†). The btrb ligands in **7** are all coordinated with three Cd(II) atoms (Fig. S26 in the ESI†). The Cd(II) atoms are connected by bpdc and btrb ligands and form a 2D network (Fig. 7a).

Topologically, each Cd1 atom links two bpdc and two btrb ligands and is 4-connected. Each Cd2 atom connects one btrb ligand and three bptc ligands and is 4-connected (Fig. S27 in the ESI†). The bpdc (O1–O4) and btrb ligands are 3-connected. The bpdc ligand (O5–O8) is 2-connected. The 2D network of **7** can be simplified as a (3,3,4,4)-connected 2D 3,3,4,4L72 network with a point symbol of $(3{\cdot}4{\cdot}5)(4{\cdot}8^2)(3{\cdot}4{\cdot}5{\cdot}8^3)(3{\cdot}4{\cdot}8^2{\cdot}9^2)$ (Fig. 7b).[21]

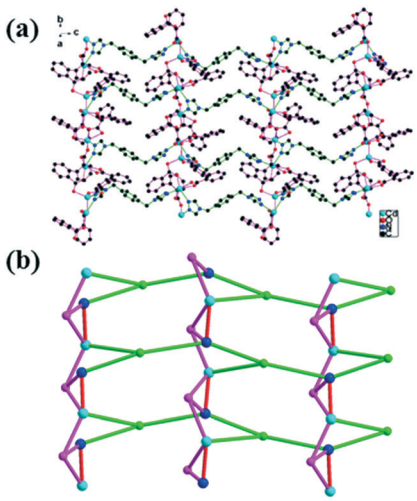

Fig. 7 (a) The 2D network in **7**; (b) schematic depiction of the (3,3,4,4)-connected network in **7**. The bright green, pink, blue and turquoise balls represent the 3-connected btrb ligands, 3-connected bpdc (O5–O8) ligands, 4-connected Cd1 atoms and 4-connected Cd2 atoms, respectively. The red sticks represent 2-connected bpdc ligands (O5–O8).

Crystal structure of $\{[Cd(btrb)(bpdc)]{\cdot}H_2O\}_n$ (8)

8 shows a (3,5)-connected 2D network. The asymmetric unit of **8** consists of half of a Cd(II) atom, half of a btrb ligand, half of a bpdc ligand and half of a disordered lattice water molecule. Cd1 is in a slightly distorted octahedral geometry coordinated with four carboxylate oxygen atoms (O1/O1A/O2B/O2C) from three bpdc ligands and two nitrogen atoms (N1/N1A) from two btrb ligands (Fig. S28 in the ESI†). The bpdc ligands in **8** show a dual bidentate coordination mode and link three Cd(II) atoms (O1O2/O1AO2A) (Fig. S29 in the ESI†). The btrb ligands exhibit an *anti*-configuration and are 2-connected with their 1-position triazole nitrogen atoms. The Cd(II) atoms are connected by bpdc and btrb ligands to construct a 2D network (Fig. 8a).

Topologically, each Cd(II) atom links three bpdc ligands and two btrb ligands and is 5-connected (Fig. S30 in the ESI†). Each bpdc ligand is 3-connected. Each btrb ligand is 2-connected. The 2D network of **8** can be simplified as a (3,5)-connected self-catenated 2D 3,5L2 network with a point symbol of $(4^2{\cdot}6)(4^2{\cdot}6^7{\cdot}8)$ (Fig. 8b).[21]

Effects of multicarboxylate ligands and the bis(triazole) ligand btrb on the structures of 1–8

In this work, we used Cd(II) as the metal centre, the btrb ligand as the main ligand, and different carboxylate ligands as the auxiliary ligands to tune the structures of the CPs **1–8**.

Initially, we chose 1,2,4,5-benzenetetracarboxylic acid (H_4-btec) as an auxiliary ligand, thus the unprecedented (4,4,4,4)-connected 3D (electroneutral motif) + 1D (cationic motif) → 3D polythreaded structure of **1** was obtained. The unprecedented 3D (4,5,6)-connected structure of **2** was synthesized if the tetracarboxylate ligand btec was replaced by (1,1′-

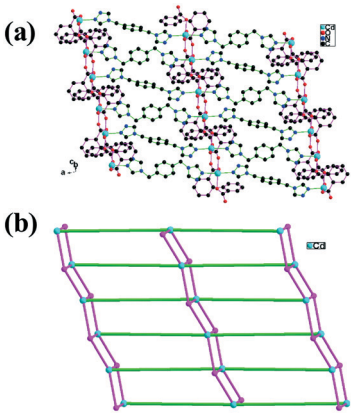

Fig. 8 (a) The 2D structure of **8**. (b) Schematic depiction of the (3,5)-connected 2D network of **8**. The turquoise and pink balls represent the 5-connected Cd atoms and 3-connected bpdc ligands, respectively. The bright green sticks represent the 2-connected btrb ligands.

Open Access Article. Published on 11 September 2017. Downloaded on 12/4/2025 7:41:17 PM.
This article is licensed under a Creative Commons Attribution-NonCommercial 3.0 Unported Licence.

biphenyl)tetracarboxylic acid (H_4bptc). When the tricarboxylate ligand 1,3,5-benzenetricarboxylic acid (H_3btc) was used, an unprecedented 3D (3,8)-connected topology of **3**, based on the Cd(II) trimer cluster [$Cd_3(COO)_2$], was obtained. If the dicarboxylic ligand isophthalic acid (H_2ip) was used, **4** exhibited a 2D + 2D → 2D interpenetration network based on the 2D **sql** network. **5** exhibited a 4-connected 3D **cds** network when the dicarboxylic ligand 4-methoxyl-isophthalic acid (H_2MeOip) was used. **6** presented the first 2-fold interpenetrating **cco-6-*Pbcm*** 3D network when the dicarboxylic ligand phthalic acid (1,2-H_2bdc) was used. A (3,3,4,4)-connected 2D network of **7** and a (3,5)-connected self-catenated 2D network of **8** were synthesized when the dicarboxylic ligand (1,1′-biphenyl)-2,2′-dicarboxylic acid (H_2bpdc) was used.

The carboxyl in **1–8** shows five kinds of coordination mode: monodentate, chelating, bidentate, monodentate bridging and chelating bridging (Fig. S31 in the ESI†). The *ortho*-position carboxyl of the 1,2-bdc, btec and bptc ligands makes them easier to chelate with more Cd(II) atoms compared with the *meta*-position carboxyl of the ip and MeOip ligands. The Cd(II) atoms are more aggregated in **1**, **2** and **6** than in **4** and **5**. Due to the formation of $Cd_3(COO)_2$, the Cd(II) atoms in **3** are the most concentrated. This result suggests an advantage of multidentate ligands in the formation of metal clusters. The coordination modes of the carboxylate ligands and btrb ligands in **4** and **5** are very similar but their structures are quite different. **4** is a typical 2D 'wave' **sql** network, while **5** is a 4-connected 3D **cds** network with a point symbol of (6^5·8). The steric hindrance effect of the 4-substituent group in MeOip during assembly may be the main reason for the difference between **4** and **5**. One bptc ligand is the combination of two 1,2-bdc ligands. The bigger molecular volume of bptc may limit the coordination of btrb ligands. More btrb ligands join in the coordination in **6** than in **2**. The addition of different amounts of bpdc ligands results in the formation of **7** and **8**. The formulae of **7** and **8** show the phenomenon that the fewer bpdc ligands are added, the more btrb ligands join in coordination. These cases show the competition effect in co-ligand systems. **1–8** show the topologies devisable by the regulation of multicarboxylate ligands.

The btrb ligand was expected to be tetradentate since it has four donor nitrogen atoms. Indeed, this coordination mode (μ_4) is typical; it occurs in complexes **1**, **2**, **3** and **6**. However, the simple bridging mode μ_2 is also quite ordinary; it is found in complexes **4**, **5**, **6** and **8**. The intermediate μ_3 mode is realized only in **7**. Thus, the btrb ligand shows three kinds of coordination mode (Fig. S32 in the ESI†). The μ_3 and μ_4 modes result in the formation of condensed polynuclear groups of Cd atoms connected by N–N bridges: in **1** and **6** such groups are represented by dimers, in **3** – trimers, and in **2** – chains (Fig. S33 in the ESI†).

Despite rather simple coordination modes, the btrb ligand provides a diverse range of coordination network topologies. Some of them are rare, like **mot**, which, according to the ToposPro TTO Collection,[8a] is found only in [(μ_4-isophthalato)$_2$(μ_3-isophthalato)$_2$(1,10-phenanthroline)$_3$Dy$_3$-(NO_3)]·2H_2O (CEJBEA)[22] or 3,3,4,4L72, which is realized only in [(1,3-propanediamine)$_3$Cu$_3$W$_2$(CN)$_{18}$]·3H_2O (IRIRIK),[24] while others are unique, like *bli2* and *bli3*. Complex **6** is also unique as it is the first example of a 2-fold **cco-6-*Pbcm*** topology. Importantly, in all these cases the btrb ligand forms condensed groups (Fig. S33 in the ESI†); when it plays the role of a bridge, the topologies become quite common, like in **4** (**sql**) and **8** (3,5L2).

Another important feature of the btrb ligand is that it provides a plethora of catenation (self-catenation in **3** and **8** or interpenetration in **4** and **6**). This is obviously caused by its length and twisted geometry.

Thus, the btrb ligand demonstrates a way to obtain new architectures of coordination polymers: the ligand should be polydentate and plays two roles: as a linker in polynuclear complex groups and as a bridge between them. A complicated geometrical form and stretching will lead to catenated topologies.

Solid state photoluminescence properties

The solid-state luminescence spectra of **1–8** were studied at room temperature. The free btrb ligand does not show luminescent properties in the solid state. The possible btrb fluorescence through intra-ligand charge transfer is apparently quenched by the thermal intra-ligand rotations around the C–C and C–N bonds.[15a,25] **1–8** have emission band maxima at 444 and 469 nm (ex = 342 nm) for **1**, 462 and 525 nm (ex = 345 nm) for **2**, 413 and 467 nm (ex = 320 nm) for **3**, 421 and 465 nm (ex = 316 nm) for **4**, 429 and 464 nm (ex = 323 nm) for **5**, 436 and 464 nm (ex = 326 nm) for **6**, 437 and 465 nm (ex = 333 nm) for **7**, and 445 and 473 nm (ex = 333 nm) for **8**, respectively (Fig. 9). Due to the d^{10} configuration, the Cd(II) ion is difficult to oxidize or reduce. The emissions are neither metal-to-ligand charge transfer (MLCT) nor ligand-to-metal charge transfer (LMCT). The emissions can be attributed to the intra-ligand and ligand-to-ligand charge transitions (LLCT) from the btrb and multicarboxylate ligands.[25]

1–8 all show two emission peaks. The free H_4btec, H_4bptc, H_3btc, H_2ip, H_2MeOip, 1,2-H_2bdc and H_2bpdc ligands exhibit emissions at 336, 402, 328, 346, 360, 354 and 364 nm,

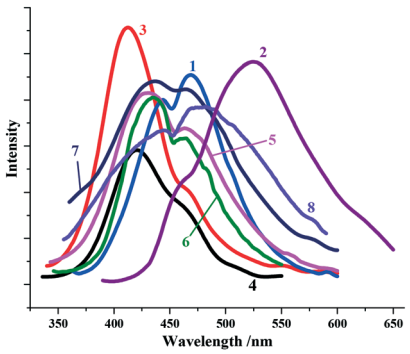

Fig. 9 The luminescence emission curves of **1–8**.

Open Access Article. Published on 11 September 2017. Downloaded on 12/4/2025 7:41:17 PM.
This article is licensed under a Creative Commons Attribution-NonCommercial 3.0 Unported Licence.

Table 1 Emission peaks of CPs **1–8** and free multicarboxylate ligands

CP	Emission peak from btrb in CP (nm)	Emission peak from carboxylate in CP (nm)	Emission peak from free carboxylate ligand (nm)	Red shift value of carboxylate in CP (nm)
1	469	444	336	108
2	462	525	402	123
3	467	413	328	85
4	465	421	346	75
5	464	429	360	69
6	464	436	354	82
7	465	437	364	73
8	473	445	364	81

respectively, which are probably attributable to the π* → n or π* → π transitions.[26] The emission peaks of **1–8** are listed in Table 1 for comparison. Fixation of the btrb ligand in a coordination network stops the rotation and freezes a single conformation to enable fluorescence; the btrb ligand may show luminescence when it coordinates with Cd(II) atoms.[25] One of the emission peaks of **1–8** is near 466 nm, which tentatively results from the btrb ligands. The two benzene rings of the bptc ligand in **2** are in the *a* plane and have the biggest conjugative effect, while other single benzene ring carboxylate ligands have similar weak conjugative systems. The two benzene rings of the bpdc ligand in **7** and **8** rotate a large angle, 65.8° and 60.0° in **7** and 63.6° in **8**. Thus, the bpdc ligands in **7** and **8** have similar conjugative effects compared with single benzene ring carboxylate ligands. The bigger conjugative effect in **2** results in the exceptional emission shift.[26c–f] $[Cd(btc)_{0.5}(phen)]\cdot H_2O$ (H_4btc = biphenyl-3,3′,4,4′-tetracarboxylic acid, phen = 1,10-phenanthroline) has an emission peak at 506 nm[26g] and $[Cd_2(bptc)(L)_2(H_2O)_2]\cdot 5H_2O$ (L = 2-(2-chloro-6-fluorophenyl)-1*H*-imidazo[4,5-*f*][1,10]-phenanthroline and H_4bptc = 3,3′,4,4′-biphenyltetracarboxylic acid) shows a similar emission peak at 518 nm.[26h] The other emission peaks of **1–8** are attributed to the n → π* or π → π* LLCT from the multicarboxylate ligands. The emissions from carboxylate ligands show different red shift values from 69 to 123 nm. The red-shift is mainly due to the coordination interactions, which effectively increase the rigidity of the ligand and reduce the loss of energy by non-radiative decay of the intra-ligand emission excited state.[25]

PXRD and thermal stability

The measured and simulated PXRDs confirm the purity of **1–8** (Fig. S34–S41 in the ESI†). Thermogravimetric analysis (TGA) of **1–8** was performed on crystalline samples heated from rt. to 800 °C in a nitrogen atmosphere (Fig. S42 in the ESI†). The water molecules of **1** were completely lost at 150 °C (calcd: 12.29%, found: 12.30%), and the framework was stable up to 220 °C. The residue of **1** at 800 °C should be CdO (calcd: 31.30%, found: 31.55%). The lattice and coordination water molecules of **2** were completely lost at 118 °C (calcd: 4.36%, found: 2.29%), and the network was stable up to 354 °C. The residue of **2** at 800 °C should be CdO (calcd: 31.04%, found: 32.07%). The lattice and coordination water molecules of **3** were completely lost at 162 °C (calcd: 5.17%, found: 4.57%), and the network was stable up to 394 °C. The residue of **3** at 800 °C should be CdO (calcd: 36.84%, found: 37.42%). The lattice and coordination water molecules of **4–8** were completely lost at 117 °C, 162 °C, 175 °C, 149 °C and 130 °C, respectively (calcd: 6.52%, found: 6.67% for **4**, calcd: 3.19%, found: 3.25% for **5**, calcd: 4.97%, found: 4.69% for **6**, calcd: 9.49%, found: 9.63% for **7** and calcd: 2.95%, found: 2.98% for **8**). The anhydrous matters of **4–8** were thermally stable up to 273 °C, 308 °C, 263 °C, 294 °C and 256 °C, respectively. Then weight loss continuously occurred and did not end until 800 °C. The main residues at 800 °C were consistent with CdO (calcd: 23.23%, found: 23.27% for **4**, calcd: 22.73%, found: 22.79% for **5**, calcd: 23.61%, found: 23.51% for **6**, calcd: 24.59%, found: 24.50% for **7** and calcd: 21.02%, found: 21.05% for **8**).

Conclusions

In short, eight Cd(II) CPs were synthesized using the flexible bis(triazole) ligand 1,4-bis(1,2,4-triazol-4-ylmethyl)benzene and seven multicarboxylate ligands under hydrothermal conditions. **1** presents an unprecedented (4,4,4,4)-connected 3D (electroneutral motif) + 1D (cationic motif) → 3D polythreaded network. **2** shows an unprecedented 3D (4,5,6)-connected structure. **3** shows an unprecedented 3D (3,8)-connected topology based on the Cd(II) trimer cluster $[Cd_3(COO)_2]$. **4** exhibits a 2D + 2D → 2D interpenetration network based on the 2D **sql** network. **5** exhibits a 4-connected **cds** 3D network. **6** presents the first 2-fold interpenetrating **cco-6-*Pbcm*** 3D network. **7** shows a (3,3,4,4)-connected 2D network. **8** presents a (3,5)-connected self-catenated 2D network with a point symbol of $(4^2\cdot 6)(4^2\cdot 6^7\cdot 8)$. The diverse structures demonstrate that the structures of coordination polymers can be successfully tuned by the carboxylate and bis(triazole) co-ligands. **1–3** show unprecedented 3D topologies. The 3D structures of **3** and **8** are self-catenated. The successful syntheses of **1–8** demonstrate that the topologies of coordination polymers can be adjusted and that unprecedented and intriguing topologies can be constructed by bis(1,2,4-triazole) and multicarboxylate co-ligands. This work contributes to the development of crystal engineering and materials science.

Conflicts of interest

There are no conflicts of interest to declare.

Acknowledgements

This work is supported by the National Natural Science Foundation of China (No. 21171126), Natural Science Foundation of Jiangsu Province (No. BK20161212), Priority Academic Program Development of Jiangsu Higher Education Institutions, State and Local Joint Engineering Laboratory for Functional Polymeric Materials and the project of scientific and

Open Access Article. Published on 11 September 2017. Downloaded on 12/4/2025 7:41:17 PM.
This article is licensed under a Creative Commons Attribution-NonCommercial 3.0 Unported Licence.

technological infrastructure of Suzhou (SZS201708). Vladislav A. Blatov is grateful to the Russian Government (Grant 14. B25.31.0005) for support.

References

1 (*a*) M. O'Keeffe and O. M. Yaghi, *Chem. Rev.*, 2012, **112**, 675; (*b*) M. Li, D. Li, M. O'Keeffe and O. M. Yaghi, *Chem. Rev.*, 2014, **114**, 1343; (*c*) J. R. Li, R. J. Kuppler and H. C. Zhou, *Chem. Soc. Rev.*, 2009, **38**, 1477; (*d*) J. R. Li, J. Sculley and H. C. Zhou, *Chem. Rev.*, 2012, **112**, 869; (*e*) J. B. DeCoste and G. W. Peterson, *Chem. Rev.*, 2014, **114**, 5695; (*f*) M. Du, C. P. Li, C. S. Liu and S. M. Fang, *Coord. Chem. Rev.*, 2013, **257**, 1282.

2 (*a*) Q. X. Han, B. Qi, W. M. Ren, C. He, J. Y. Niu and C. Y. Duan, *Nat. Commun.*, 2015, **6**, 10007; (*b*) H. L. Tang, S. C. Cai, S. L. Xie, Z. B. Wang, Y. X. Tong, M. Pan and X. H. Lu, *Adv. Sci.*, 2016, **3**, 1500265; (*c*) C. K. Wang, F. F. Xing, Y. L. Bai, Y. M. Zhao, M. X. Li and S. R. Zhu, *Cryst. Growth Des.*, 2016, **16**, 2277; (*d*) Y. J. Yang, M. J. Wang and K. L. Zhang, *J. Mater. Chem. C*, 2016, **4**, 11404.

3 (*a*) D. Liu, J. P. Lang and B. F. Abrahams, *J. Am. Chem. Soc.*, 2011, **133**, 11042; (*b*) D. Liu, Z. G. Ren, H. X. Li, J. P. Lang, N. Y. Li and B. F. Abrahams, *Angew. Chem., Int. Ed.*, 2010, **49**, 4767; (*c*) Z. Z. Lu, R. Zhang, Y. Z. Li, Z. J. Guo and H. G. Zheng, *J. Am. Chem. Soc.*, 2011, **133**, 4172; (*d*) P. Yang, X. He, M. X. Li, Q. Ye, J. Z. Ge, Z. X. Wang, S. R. Zhu, M. Shao and H. L. Cai, *J. Mater. Chem.*, 2012, **22**, 2398; (*e*) H. B. Zhou, J. H. Yao, X. P. Shen, H. Zhou and A. H. Yuan, *RSC Adv.*, 2014, **4**, 61; (*f*) S. Y. Hao, S. X. Hou, K. V. Heckeb and G. H. Cui, *Dalton Trans.*, 2017, **46**, 1951; (*g*) J. W. Cui, S. X. Hou, K. V. Heckeb and G. H. Cui, *Dalton Trans.*, 2017, **46**, 2892.

4 (*a*) X. X. Liu, C. D. Shi, C. W. Zhai, M. L. Cheng, Q. Liu and G. X. Wang, *ACS Appl. Mater. Interfaces*, 2016, **8**, 4585; (*b*) M. X. Li, Y. F. Zhang, X. He, X. M. Shi, Y. P. Wang, M. Shao and Z. X. Wang, *Cryst. Growth Des.*, 2016, **16**, 2912; (*c*) X. Zhao, X. H. Bu, Q. G. Zhai, H. Tran and P. Y. Feng, *J. Am. Chem. Soc.*, 2015, **137**, 1396; (*d*) L. L. Tan, H. Li, Y. C. Qiu, D. X. Chen, X. Wang, R. Y. Pan, Y. Wang, S. X. A. Zhang, B. Wang and Y. W. Yang, *Chem. Sci.*, 2015, **6**, 1640; (*e*) X. L. Lv, K. C. Wang, B. Wang, J. Su, X. D. Zou, Y. B. Xie, J. R. Li and H. C. Zhou, *J. Am. Chem. Soc.*, 2017, **139**, 211.

5 (*a*) J. Cepeda and A. Rodríguez-Diéguez, *CrystEngComm*, 2016, **18**, 8556; (*b*) Y. L. Li, Y. Zhao, P. Wang, Y. S. Kang, Q. Liu, X. D. Zhang and W. Y. Sun, *Inorg. Chem.*, 2016, **55**, 11821; (*c*) L. Di, J. J. Zhang, S. Q. Liu, J. Ni, H. J. Zhou and Y. J. Sun, *Cryst. Growth Des.*, 2016, **16**, 4539; (*d*) Z. C. Hu, W. P. Lustig, J. M. Zhang, C. Zheng, H. Wang, S. J. Teat, Q. H. Gong, N. D. Rudd and J. Li, *J. Am. Chem. Soc.*, 2015, **137**, 16209; (*e*) Q. Zhang, J. Su, D. W. Feng, Z. W. Wei, X. D. Zou and H. C. Zhou, *J. Am. Chem. Soc.*, 2015, **137**, 10064.

6 (*a*) S. Y. Zhang, W. Shi, P. Cheng and M. J. Zaworotko, *J. Am. Chem. Soc.*, 2015, **137**, 12203; (*b*) L. L. Zhu, C. F. Tan, M. M. Gao and G. W. Ho, *Adv. Mater.*, 2015, **27**, 7713; (*c*) S. Yuan, T. F. Liu, D. W. Feng, J. Tian, K. C. Wang, J. S. Qin, Q. Zhang, Y. P. Chen, M. Bosch, L. F. Zou, S. J. Teat, S. J. Dalgarno and H. C. Zhou, *Chem. Sci.*, 2015, **6**, 3926; (*d*) D. K. Maity, B. Bhattacharya, A. Halder and D. Ghoshal, *Dalton Trans.*, 2015, **4**, 20999; (*e*) B. Bhattacharya, A. Halder, D. K. Maity and D. Ghoshal, *CrystEngComm*, 2016, **18**, 4074.

7 http://topospro.com.

8 (*a*) V. A. Blatov, A. P. Shevchenko and D. M. Proserpio, *Cryst. Growth Des.*, 2014, **14**, 3576; (*b*) S. W. Zhang, J. G. Ma, X. P. Zhang, E. Y. Duan and P. Cheng, *Inorg. Chem.*, 2015, **54**, 586; (*c*) D. Sun, Z. H. Yan, V. A. Blatov, L. Wang and D. F. Sun, *Cryst. Growth Des.*, 2013, **13**, 1277; (*d*) X. H. Jing, X. C. Yi, E. Q. Gao and V. A. Blatov, *Dalton Trans.*, 2012, **41**, 14316; (*e*) M. Marmier, G. Cecot, A. V. Vologzhanina, J. L. Bila, I. Zivkovic, H. M. Ronnow, B. Nafradi, E. Solari, P. Pattison, R. Scopellitia and K. Severin, *Dalton Trans.*, 2016, **45**, 15507; (*f*) G. H. Cui, C. H. He, C. H. Jiao, J. C. Geng and V. A. Blatov, *CrystEngComm*, 2012, **14**, 4210; (*g*) H. Q. Ma, D. Sun, L. L. Zhang, R. M. Wang, V. A. Blatov, J. Guo and D. F. Sun, *Inorg. Chem.*, 2013, **52**, 10732.

9 (*a*) S. R. Batten and R. Robson, *Angew. Chem., Int. Ed.*, 1998, **37**, 1460; (*b*) L. Carlucci, G. Ciani and D. M. Proserpio, *Coord. Chem. Rev.*, 2003, **246**, 247; (*c*) E. V. Alexandrov, V. A. Blatov and D. M. Proserpio, *CrystEngComm*, 2017, **19**, 1993; (*d*) Y. N. Gong, D. C. Zhong and T. B. Lu, *CrystEngComm*, 2016, **18**, 2596.

10 (*a*) Y. Gong, J. Li, J. Qin, T. Wu, R. Cao and J. Li, *Cryst. Growth Des.*, 2011, **11**, 1662; (*b*) B. Xu, J. Lu and R. Cao, *Cryst. Growth Des.*, 2009, **9**, 3003; (*c*) G. P. Yang, L. Hou, L. F. Ma and Y. Y. Wang, *CrystEngComm*, 2013, **15**, 2561; (*d*) A. L. Chen, N. Liu, Y. F. Yue, Y. W. Jiang, E. Q. Gao, C. H. Yan and M. Y. He, *Chem. Commun.*, 2007, 407; (*e*) G. W. Xu, Y. P. Wu, H. B. Wang, Y. N. Wang, D. S. Li and Y. L. Lu, *CrystEngComm*, 2015, **17**, 9055; (*f*) J. M. Hu, V. A. Blatov, B. Y. Yu, K. V. Heckec and G. H. Cui, *Dalton Trans.*, 2016, **45**, 2426; (*g*) V. Martins, J. A. L. C. Resende and C. M. Ronconi, *CrystEngComm*, 2017, **19**, 3103.

11 (*a*) Q. X. Yao, Z. F. Xu, X. H. Jin and J. Zhang, *Inorg. Chem.*, 2009, **48**, 1266; (*b*) Y. Y. Liu, Z. H. Wang, J. Yang, B. Liu, Y. Y. Liu and J. F. Ma, *CrystEngComm*, 2011, **13**, 3811; (*c*) H. Y. Zang, Y. Q. Lan, G. S. Yang, X. L. Wang, K. Z. Shao, G. J. Xu and Z. M. Su, *CrystEngComm*, 2010, **12**, 434; (*d*) B. Zheng and J. Bai, *CrystEngComm*, 2009, **11**, 271; (*e*) G. H. Wang, Z. G. Li, H. Q. Jia, N. H. Hu and J. W. Xu, *Cryst. Growth Des.*, 2008, **8**, 1932; (*f*) X. Y. Cao, Q. P. Lin, Y. Y. Qin, J. Zhang, Z. J. Li, J. K. Cheng and Y. Y. Yao, *Cryst. Growth Des.*, 2009, **9**, 20; (*g*) H. Wu, B. Liu, J. Yang, H. Y. Liu and J. F. Ma, *CrystEngComm*, 2011, **13**, 3661.

12 (*a*) Y. Q. Lan, S. L. Li, Z. M. Su, K. Z. Shao, J. F. Ma, X. L. Wang and E. B. Wang, *Chem. Commun.*, 2008, 58; (*b*) Y. Q. Lan, S. L. Li, X. L. Wang, K. Z. Shao, D. Y. Du, H. Y. Zang and Z. M. Su, *Inorg. Chem.*, 2008, **47**, 8179; (*c*) J. X. Meng, Y. Lu, Y. G. Li, H. Fu and E. B. Wang, *Cryst. Growth Des.*, 2009, **9**, 4116; (*d*) Y. F. Cui, X. Qian, Q. Chen, B. L. Li and H. Y. Li, *CrystEngComm*, 2012, **14**, 1201; (*e*) M. Li, S. Zhao, Y. F. Peng, B. L. Li and H. Y. Li, *Dalton Trans.*, 2013, **42**,

Open Access Article. Published on 11 September 2017. Downloaded on 12/4/2025 7:41:17 PM.
This article is licensed under a Creative Commons Attribution-NonCommercial 3.0 Unported Licence.

9771; (*f*) M. Li, Y. F. Peng, S. Zhao, B. L. Li and H. Y. Li, *RSC Adv.*, 2014, **4**, 14241.

13 (*a*) B. Zheng, H. Dong, J. F. Bai, Y. Z. Li, S. H. Li and M. Scheer, *J. Am. Chem. Soc.*, 2008, **130**, 7778; (*b*) D. K. Maity, A. Halder, B. Bhattacharya, A. Das and D. Ghoshal, *Cryst. Growth Des.*, 2016, **16**, 1162; (*c*) M. Chen, Y. Lu, J. Fan, G. C. Lv, Y. Zhao and W. Y. Sun, *CrystEngComm*, 2012, **44**, 2015; (*d*) R. Luo, H. Xu, H. X. Gu, X. Wang, Y. Xu, X. Shen, W. W. Bao and D. R. Zhu, *CrystEngComm*, 2014, **16**, 784; (*e*) Y. Zhang, J. Yang, Y. Yang, J. Guo and J. F. Ma, *Cryst. Growth Des.*, 2012, **12**, 4060; (*f*) Z. Su, M. Chen, T. Okamura, M. S. Chen, S. S. Chen and W. Y. Sun, *Inorg. Chem.*, 2011, **50**, 985; (*g*) S. L. Li, K. Tan, Y. Q. Lan, J. S. Qin, M. N. Li, D. Y. Du, H. Y. Zang and Z. M. Su, *Cryst. Growth Des.*, 2010, **10**, 1699; (*h*) J. B. Lin, J. P. Zhang, W. X. Zhang, W. Xue, D. X. Xue and X. M. Chen, *Inorg. Chem.*, 2009, **48**, 6652; (*i*) C. P. Li and M. Du, *Chem. Commun.*, 2011, **47**, 5958; (*j*) L. Q. Ma and W. B. Lin, *J. Am. Chem. Soc.*, 2008, **130**, 13834; (*k*) R. Peng, S. R. Deng, M. Li, D. Li and Z. Y. Li, *CrystEngComm*, 2008, **10**, 590; (*l*) D. L. Michael and D. B. Paul, *Coord. Chem. Rev.*, 2006, **250**, 3142; (*m*) P. A. Gale, M. E. Light and R. Quesada, *Chem. Commun.*, 2005, 5864.

14 (*a*) G. A. Senchyk, A. B. Lysenko, H. Krautscheid, E. B. Rusanov, A. N. Chernega, K. W. Krämer, S. X. Liu, S. Decurtins and K. V. Domasevitch, *Inorg. Chem.*, 2013, **52**, 863; (*b*) J. H. Zhou, R. M. Cheng, Y. Song, Y. Z. Li, X. T. Chen, Z. L. Xue and X. Z. You, *Inorg. Chem.*, 2005, **44**, 8011; (*c*) E. C. Yang, B. Ding, Z. Y. Liu, Y. L. Yang and X. J. Zhao, *Cryst. Growth Des.*, 2012, **12**, 1185; (*d*) H. A. Habib, J. Sanchiz and C. Janiak, *Inorg. Chim. Acta*, 2009, **362**, 2452; (*e*) Y. X. Shi, F. L. Hu, W. H. Zhang and J. P. Lang, *CrystEngComm*, 2015, **17**, 9404; (*f*) L. Qin, L. N. Wang, P. J. Ma and G. H. Cui, *J. Mol. Struct.*, 2014, **1059**, 202; (*g*) L. L. Liu, C. X. Yu, F. J. Ma, Y. R. Li, J. J. Han, L. Lin and L. F. Ma, *Dalton Trans.*, 2015, **44**, 1636; (*h*) X. X. Wang, B. Y. Yu, K. V. Hecke and G. H. Cui, *RSC Adv.*, 2014, **4**, 61281; (*i*) N. N. Adarsh, P. Sahoo and P. Dastidar, *Cryst. Growth Des.*, 2010, **10**, 4976; (*j*) M. H. Mir, S. Kitagawa and J. J. Vittal, *Inorg. Chem.*, 2008, **47**, 7728; (*k*) G. H. Cui, C. H. He, C. H. Jiao, J. C. Geng and V. A. Blatov, *CrystEngComm*, 2012, **14**, 4210; (*l*) S. Q. Zang, M. M. Dong, Y. J. Fan, H. W. Hou and T. C. W. Mak, *Cryst. Growth Des.*, 2012, **12**, 1239; (*m*) Q. Chu, Z. Su, J. Fan, T. Okamura, G. C. Lv, G. X. Liu, W. Y. Sun and N. Ueyama, *Cryst. Growth Des.*, 2011, **11**, 3885.

15 (*a*) J. G. Ding, X. Zhu, Y. F. Cui, N. Liang, P. P. Sun, Q. Chen, B. L. Li and H. Y. Li, *CrystEngComm*, 2014, **16**, 1632; (*b*) S. S. Han, L. L. Shi, K. Li, S. Zhao, B. L. Li and B. Wu, *RSC Adv.*, 2015, **5**, 107166; (*c*) Y. F. Peng, S. Zhao, K. Li, L. Liu, B. L. Li and B. Wu, *CrystEngComm*, 2015, **17**, 2544; (*d*) K. Li, X. X. Lv, L. L. Shi, L. Liu, B. L. Li and B. Wu, *Dalton Trans.*, 2016, **45**, 15078; (*e*) L. Liu, Y. F. Peng, X. X. Lv, K. Li, B. L. Li and B. Wu, *CrystEngComm*, 2016, **18**, 2490; (*f*) S. Zhao, X. X. Lv, L. L. Shi, B. L. Li and B. Wu, *RSC Adv.*, 2016, **6**, 56035; (*g*) X. X. Lv, L. L. Shi, K. Li, B. L. Li and H. Y. Li, *Chem. Commun.*, 2017, **53**, 1860; (*h*) L. L. Shi, T. R. Zheng, M. Li, L. L. Qian, B. L. Li and H. Y. Li, *RSC Adv.*, 2017, **7**, 23432.

16 (*a*) C. R. Murdock, N. W. McNutt, D. J. Keffer and D. M. Jenkins, *J. Am. Chem. Soc.*, 2014, **136**, 671; (*b*) R. M. Christopher and M. J. David, *J. Am. Chem. Soc.*, 2014, **136**, 10983.

17 (*a*) R. Jacobson, *Private communication to the Rigaku Corporation*, Tokyo, Japan, 1998;; (*b*) *CrysAlisPro*, Agilent Technologies, Version 1.171.36.32 (release 02-08-2013 CrysAlis171.NET);; (*c*) L. Krause, R. Herbst-Irmer, G. M. Sheldrick and D. Stalke, *J. Appl. Crystallogr.*, 2015, **48**, 3.

18 (*a*) G. M. Sheldrick, *Acta Crystallogr., Sect. A: Found. Crystallogr.*, 2008, **64**, 112; (*b*) G. M. Sheldrick, *Acta Crystallogr., Sect. C: Cryst. Struct. Commun.*, 2015, **71**, 3.

19 A. L. Spek, *Acta Crystallogr., Sect. A: Found. Crystallogr.*, 1990, **46**, 194.

20 Y. Q. Sun, J. Zhang and G. Y. Yang, *J. Coord. Chem.*, 2004, **57**, 1299.

21 (*a*) V. A. Blatov, M. O'Keeffe and D. M. Proserpio, *CrystEngComm*, 2010, **12**, 44; (*b*) E. V. Alexandrov, V. A. Blatov, A. V. Kochetkova and D. M. Proserpio, *CrystEngComm*, 2011, **13**, 3947; (*c*) M. O'Keeffe and O. M. Yaghi, *Chem. Rev.*, 2012, **112**, 675; (*d*) V. A. Blatov, A. P. Shevchenko and D. M. Proserpio, *Cryst. Growth Des.*, 2014, **14**, 3576.

22 P. Wang, R. Q. Fan, Y. L. Yang, X. R. Liu, W. W. Cao and B. Yang, *J. Solid State Chem.*, 2012, **196**, 441.

23 (*a*) S. Z. Zhan, D. Li, X. P. Zhou and X. H. Zhou, *Inorg. Chem.*, 2006, **45**, 9163; (*b*) S. Z. Zhan, M. Li, X. P. Zhou, J. Ni, X. C. Huang and D. Li, *Inorg. Chem.*, 2011, **50**, 8879.

24 D. F. Li, L. M. Zheng, X. Y. Wang, J. Huang, S. Gao and W. X. Tang, *Chem. Mater.*, 2003, **15**, 2094.

25 (*a*) H. A. Habib, J. Sanchiz and C. Janiak, *Inorg. Chim. Acta*, 2009, **362**, 2452; (*b*) M. D. Allendorf, C. A. Bauer, R. K. Bhakta and R. J. T. Houk, *Chem. Soc. Rev.*, 2009, **38**, 1330; (*c*) X. L. Wang, Y. F. Bi, H. Y. Lin and G. C. Liu, *Cryst. Growth Des.*, 2007, **7**, 1086; (*d*) R. Sun, Y. Z. Li, J. F. Bai and Y. Pan, *Cryst. Growth Des.*, 2007, **7**, 890; (*e*) X. W. Wang, J. Z. Chen and J. H. Liu, *Cryst. Growth Des.*, 2007, **7**, 1227; (*f*) X. L. Wang, C. Qin, E. B. Wang, L. Xu, Z. M. Su and C. W. Hu, *Angew. Chem., Int. Ed.*, 2004, **43**, 5036; (*g*) H. Yersin and A. Vogler, *Photochemistry and Photophysics of Coordination Compounds*, Springer, Berlin, 1987;; (*h*) B. Valeur, *Molecular Fluorescence: Principles and Application*, Wiley-VCH, Weinheim, 2002.

26 (*a*) Q. Y. Huang, T. Li and X. R. Meng, *Inorg. Chem. Commun.*, 2014, **49**, 52; (*b*) C. C. Wang, H. P. Jing, P. Wang and S. J. Gao, *J. Mol. Struct.*, 2015, **1080**, 44; (*c*) R. H. Cui, G. J. Xu and Z. H. Jiang, *J. Coord. Chem.*, 2011, **64**, 222; (*d*) F. Wang, X. H. Ke, J. B. Zhao, K. J. Deng, X. K. Leng, Z. F. Tian, L. L. Wen and D. F. Li, *Dalton Trans.*, 2011, **40**, 11856; (*e*) H. Wang, F. Y. Yi, S. Wang, W. G. Tian and Z. M. Sun, *Cryst. Growth Des.*, 2014, **14**, 147; (*f*) G. X. Liu, K. Zhu, H. Chen, R. Y. Huang and X. M. Ren, *Z. Anorg. Allg. Chem.*, 2009, **635**, 156; (*g*) J. J. Wang, M. L. Yang, H. M. Hua, G. L. Xue, D. S. Li and Q. Z. Shi, *Z. Anorg. Allg. Chem.*, 2007, **633**, 341; (*h*) Z. L. Xu, F. Y. Liu, Y. Xu, J. Wang, Y. Li and X. Y. Wang, *Chin. J. Struct. Chem.*, 2014, **33**, 1516.

 This journal is © The Royal Society of Chemistry 2017